Supplementary Information

Table of Contents

1. Materials and Methods

Reagents. All solutions were made using DNAse/protease-free water purchased from FisherScientific. Synthesized oligonucleotides were obtained from Integrated DNA Technologies, Inc (Coralville, IA) and concentrations of oligonucleotide stock solutions were quantified via absorbance at 260 nm on a ThermoScientific NanoDrop One (Waltham, MA).

Duplex Calibration Curve. Each molecular beacon probe was annealed with its complement by heating to 95 °C in 2 L of water for 5 minutes and cooled overnight. The MB probe and analyte were combined at 100 nM with a total volume of 1 mL. A calibration curve was then created by measuring the fluorescence for a range of duplex concentrations. The best-fit line was used to find the concentration of probe:analyte from the fluorescent intensity. Unless otherwise specified, all hybridization assays were performed with 50 mM Tris-HCl, 50 mM $MgCl_2$, 0.1% Tween-20, and pH 7.4.

Kinetics Assays. Solutions containing hybridization buffer and molecular beacon probes were placed into a Cary Agilent Fluorimeter with λ_{ex} = 485 nm and λ_{em} = 517 nm and excitation and emission slit widths each at 10 nm. After reading the baseline for 60 seconds (MB1 and MB1-Tail) or 30 seconds (τMB or τTailMB), 50 nM of the respective analyte was added and mixed, and measurements were resumed after 10 sec. The temperature was kept at 22 °C using a Single Cell Peltier attachment.

Native Polyacrylamide Gel Electrophoresis. A 12% Native PAGE was created with 50 mM $MgCl_2$, and run in TBE at 80V for 85 minutes before staining with GelRed.

Table S1. Oligonucleotides used in the study

Name	Sequence 5' ✂ 3'[a-,f]
MB1-Tail	CGT CCG CCA C /iFluorT/ CCGT CAG CGA AGC AGC ACGG /3BHQ_1/
MB1	/FAM/ CCG TCA GCG AAG CAG CAC GG /3BHQ_1/
16S-60 WT	GTC GAA CGG TAA CAG GAA GCA GCT TGC TGC TTC GCT GAC G A GTG GCG G ACG GGT GAG TAA
16S-60 C/T	GTC GAA CGG TAA CAG GAA GCA GCT TGC TGC TTT GCT GAC G A GTG GCG G ACG GGT GAG TAA
16S-60 G/T	GTC GAA CGG TAA CAG GAA GCA GCT TGC TTC TTCGCT GAC G A GTG GCG G ACG GGT GAG TAA
16S-60 (s-1)	GTC GAA CGG TAA CAG CAA GCA GCT TGC TGC TTG GCT GAC G A GTG GCG G ACG GGT GAG TAA
16S-60 mut (s-2)	GTC GAA CGG TAA CAG CTA GCA GCT TGC TGC TAG GCT GAC G A GTG GCG G ACG GGT GAG TAA
16S-60 mut (s-3)	GTC GAA CGG TAA CAG CTT GCA GCT TGC TGC AAG GCT GAC G A GTG GCG G ACG GGT GAG TAA
16S-60 (t-1)	GTC GAA CGG TAA CAG GAA GCA GCT TGC TGC TTC GCT GAC G A GTG ACG G ACG GGT GAG TAA

16S-60 (t-2)	GTC GAA CGG TAA CAG GAA GCA GCT TGC TGC TTC GCT GAC G A GTA ACG G ACG GGT GAG TAA
16S-60 (t-3)	GTC GAA CGG TAA CAG GAA GCA GCT TGC TGC TTC GCT GAC G A GAA ACG G ACG GGT GAG TAA
16S-16 WT	TGC TGC TTC GCT GAC G
16S-16 C/T	TGC TGC TTT GCT GAC G
16S-16 G/T	TGC TTC TTC GCT GAC G
16S-36	TGC TGC TTC GCT GAC G A GTG GCG G ACG GGT GAG TAA
16S-27	TGC TGC TTC GCT GAC G A GTG GCG G ACG
16S T*	GTC GAA CGG TAA CAG GAA GCA GCT TGC TGC TTC GCT GAC G **A GTG GCG G ACG**
16S T1*	GTC GAA CGG TAA CAG GAA GCA GCT TGC TGC TTC GCT GAC G **A GTG GCG G**
16S T2*	GTC GAA CGG TAA CAG GAA GCA GCT TGC TGC TTC GCT GAC G **A GTG G**
16S T3*	GTC GAA CGG TAA CAG GAA GCA GCT TGC TGC TTC GCT GAC G **A G**
16S T4	GTC GAA CGG TAA CAG GAA GCA GCT TGC TGC TTC GCT GAC G
τMB-Tail	GAC GTTT GA AGG T^{FAM} CCGC **TAC TCA CAC TGC CGC** GCGG /3BHQ_1/
τMB	**FAM**-CCGC **TAC TCA CAC TGC CGC** GCGG/**3BHQ_1/**
τ-17 WT	GCG GCA GTG TGA GTA **CC**
τ-17 0C	GCG GCA GCG TGA GTA **CC**
τ-17 1A	GCG GCA **A**TG TGA GTA **CC**
τ-60 WT	CA AAC ACG TCC CGG GAG GCG GCA GTG TGA GTA CCT TCA C AC GTC CCA TGC GCC GTG CTG T
τ-60 0C	CA AAC ACG TCC CGG GAG GC G GCA G**C**G TGA GTA CCT TCA C AC GTC CCA TGC GCC GTG CTG T
τ-60 1A	CA AAC ACG TCC CGG GAG GCG GCA **A** TG TGA GTA CCT TCA C AC GTC CCA TGC GCC GTG CTG T

***Nucleotides green and in bold letters represent those complementary to the tail of MB1-Tail**

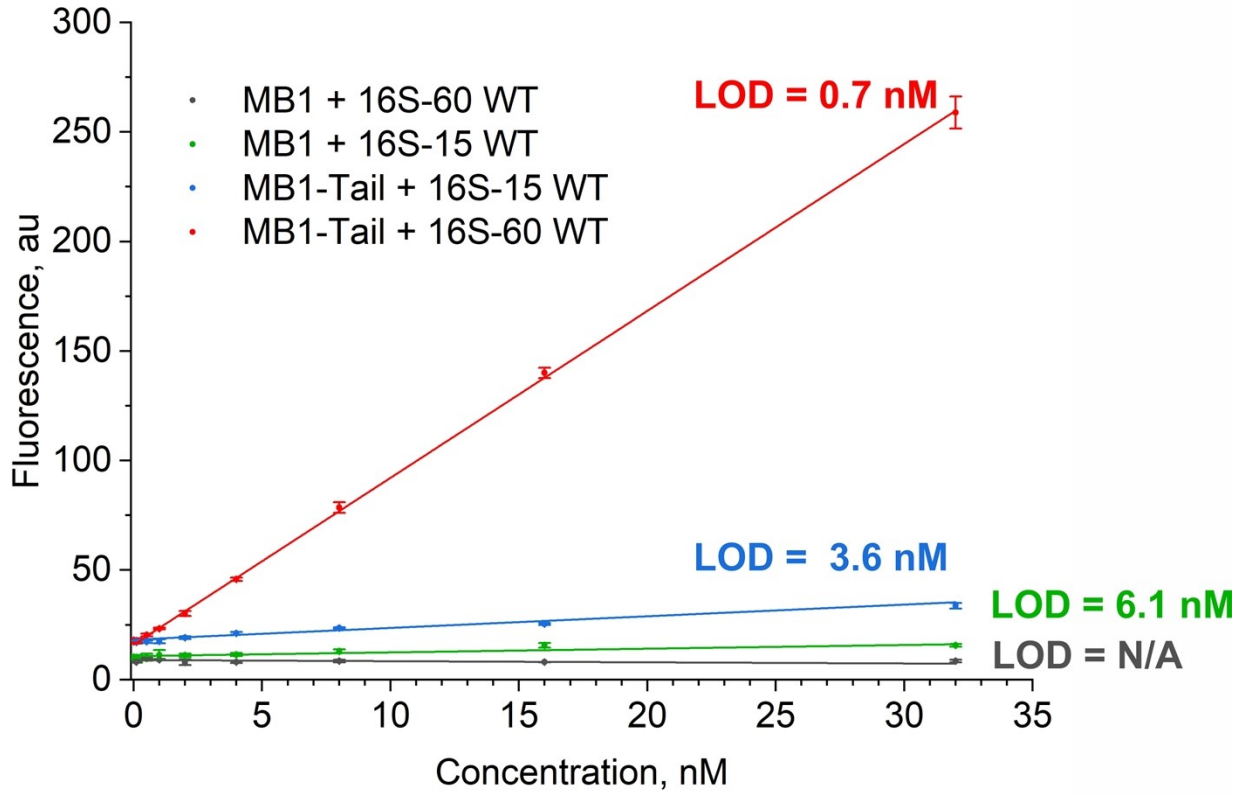

Equation	y = a + b*x			
Plot	MB1 + 16S-60 WT	MB1 + 16S-15 WT	MB1-Tail + 16S-15 WT	MB1-Tail + 16S-60 WT
Intercept	8.9 ± 0.3	10.7 ± 0.3	18.2 ± 0.6	16.0 ± 0.3
Slope	-0.05 ± 0.02	0.17 ± 0.02	0.53 ± 0.07	7.62 ± 0.11
Pearson's r	-0.71	0.95	0.95	1.00
R-Square (COD)	0.50	0.89	0.90	1.00
Adj. R-Square	0.43	0.88	0.89	1.00

Figure S1 Limit of Detection for MB1 and MB1-Tail with long and short 16S analytes. A calibration curve was used to determine the Limit of Detection (LOD) for each analyte by finding the line of best fit. To determine LOD, the average signal of the blank (F_0) was added to three times the blank's standard deviation (SD), and this value was used in the line of best fit to solve for x, the lowest detectable concentration of the analyte.

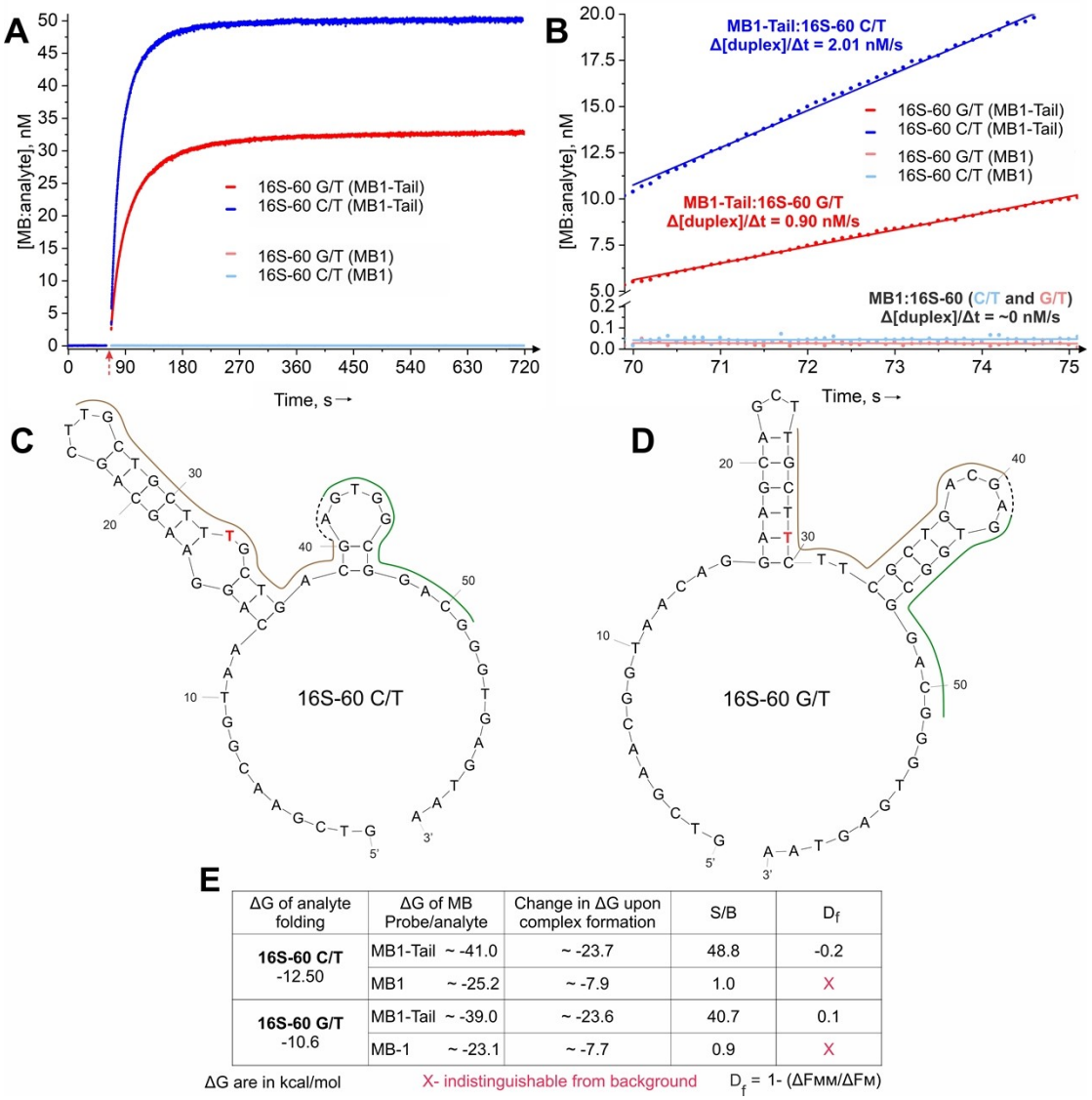

E

ΔG of analyte folding	ΔG of MB Probe/analyte	Change in ΔG upon complex formation	S/B	D_f
16S-60 C/T -12.50	MB1-Tail ~ -41.0	~ -23.7	48.8	-0.2
	MB1 ~ -25.2	~ -7.9	1.0	X
16S-60 G/T -10.6	MB1-Tail ~ -39.0	~ -23.6	40.7	0.1
	MB-1 ~ -23.1	~ -7.7	0.9	X

ΔG are in kcal/mol X- indistinguishable from background D_f = 1- (ΔFмм/ΔFм)

Figure S2. Tailed MB Probe Improves Hybridization Kinetics to Folded 16S Mutant Analytes. (A) The time-dependent hybridization kinetics between analytes and MB1 or MB1-Tail were measured. The analytes were added at the 60s time point, and measurements were resumed at ~70 s, as indicated by the red arrow. The MB:Analyte duplex concentration was determined using a line of best fit from a calibration curve (Fig. S13) **(B)** Initial hybridization rates of 16S analyte with MB1 and MB1-Tail. The line of best fit was used to determine the slope over the first 5 seconds and was taken to be the initial rate of duplex formation. **(C)** The secondary structure of the 16S-60 C/T and (D) 16S-60 G/T analyte, with mutated nucleotides in red. The brown outline indicates the binding region of the MB probe and the green outline indicates the binding region of the tail. **(E)** Free energy values and quantitative data for the analytes. The Gibbs energy values (ΔG) were obtained at 22 °C, [Na^+] = 50 mM, and the [Mg^{2+}] = 50 mM using Mfold.The signal to background was determined by taking the ratio of MB probe fluorescence in the presence of the analyte divided by the fluorescence of just the MB probe in a hybridization buffer following a 30-minute incubation (50 nM MB, 100 nM analytes). The

differentiation factor was used to determine the differentiation of wild-type from mutant analyte and the equation used was Df = 1 − ΔFmm/ΔFm, where ΔF represents the signal of matched (m) or mismatched (mm) analyte with the signal of the blank (no analyte) subtracted.

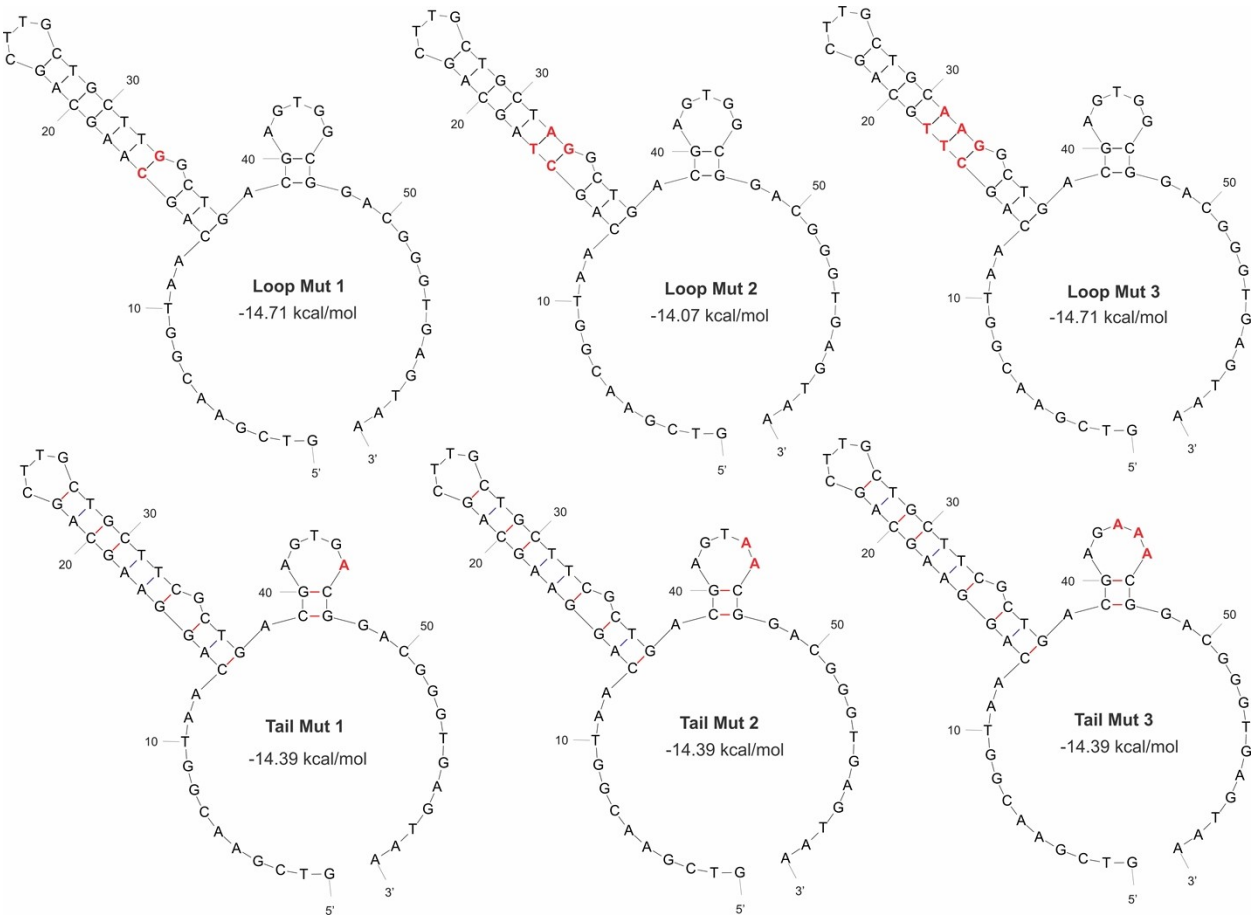

Figure S3. Secondary Structures Of 16S-60 Used In The Evaluation For Impact On MB1-Tail Regions. In the loop mutants (Loop Mut 1-3), the mutations emboldened in red were introduced such that the secondary structure was unaltered, but a mismatch to the MB stem loop was present. In the tail mutants (Tail Mut 1-3), mismatches were introduced such that the secondary structure of the analyte was unaltered, but the complementarity to the tail of the MB1-Tail probe was reduced.

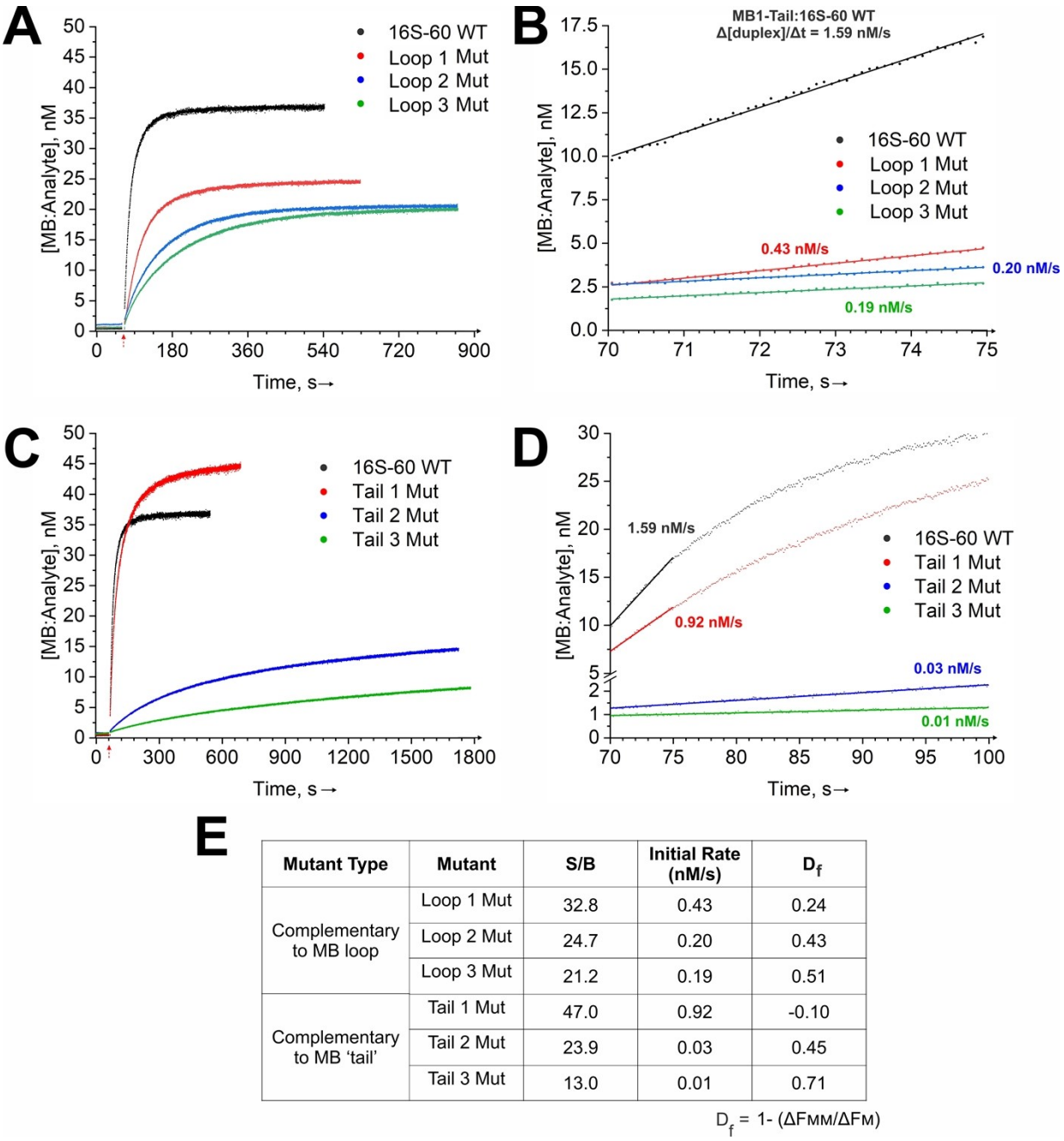

E

Mutant Type	Mutant	S/B	Initial Rate (nM/s)	D_f
Complementary to MB loop	Loop 1 Mut	32.8	0.43	0.24
	Loop 2 Mut	24.7	0.20	0.43
	Loop 3 Mut	21.2	0.19	0.51
Complementary to MB 'tail'	Tail 1 Mut	47.0	0.92	-0.10
	Tail 2 Mut	23.9	0.03	0.45
	Tail 3 Mut	13.0	0.01	0.71

D_f = 1- (ΔFMM/ΔFM)

Figure S4. Stem and Tail Mutant 16S Analyte Performance with MB1-Tail. (A) Time-dependent fluorescent duplex formation between 50 nM of MB probes and 100 nM of 16S analytes, either wild-type (WT) or with a mutation in the stem **(Fig. S10).** The analytes were added at the 60 s time point, indicated by the red arrow, and readings began again at ~70 s. **(B)** Initial hybridization rates of analytes with MB1 and MB1-Tail. A line of best fit was determined over the first 5 seconds after analyte addition, and the slope was taken to be the initial rate of duplex formation. **(C)** Similar to Panel A, but with analytes containing a mutation in the tail-binding region. **(D)** The initial rate of duplex formation was determined similarly to Panel B, but

the rate for both the Tail 2 Mutant and Tail 3 Mutant were determined over 30 s due to an unobservable increase in the first 5 s.

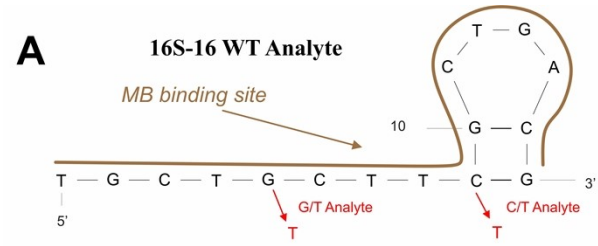

B

ΔG of analyte folding	ΔG of MB Probe/analyte	Change in ΔG upon complex formation	S/B	Initial Rate (nM/s)	D_f
16S-16 WT -1.04	MB1-Tail ~ -28.0	~ -22.2	5.2	0.007	—
	MB1 ~ -28.0	~ -22.2	6.8	0.002	—
16S-16 G/T -1.04	MB1-Tail ~ -24.2	~ -18.4	4.4	0.006	0.2
	MB1 ~ -24.2	~ -18.4	8.0	0.002	-0.2
16S-16 C/T -1.41	MB1-Tail ~ -22.2	~ -16.0	5.0	0.004	0.1
	MB1 ~ -22.2	~ -16.0	4.9	0.001	0.3

ΔG are in kcal/mol

D_f = 1- (ΔFмм/ΔFм)

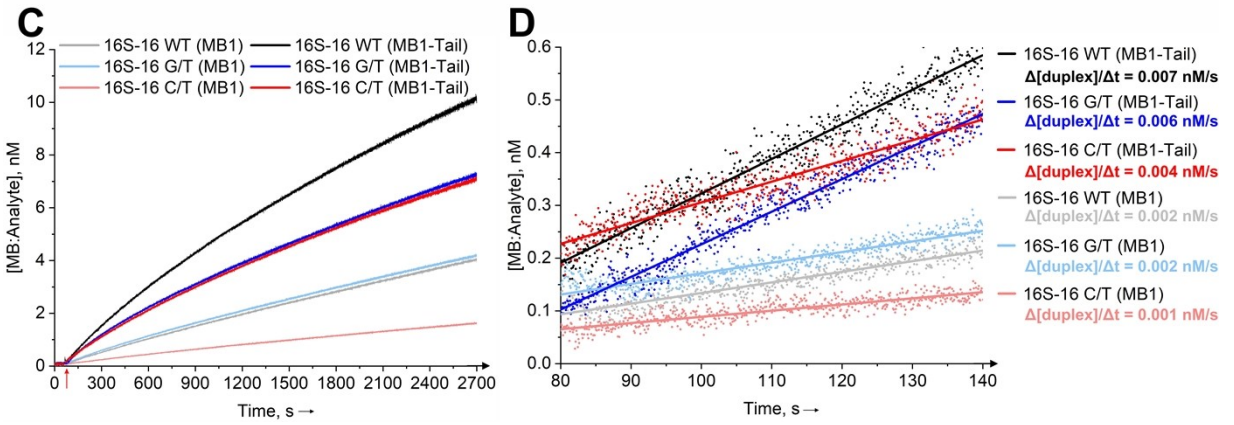

Figure S5. Kinetics and quantitative data for 16-nt linear fragments of 16S analytes. (A) The secondary structure of the 16S-16 WT analyte, with red arrows indicating the position of mutants G/T and C/T. The brown outline indicates the binding region of the MB probe and encompasses the entire analyte sequence. **(B)** Free energy values and quantitative data for the analytes. The Gibbs energy values (ΔG) were obtained at 22 °C, $[Na^+]$ = 50 mM, and the $[Mg^{2+}]$ = 50 mM using Mfold.The signal to background was determined by taking the ratio of MB probe fluorescence in the presence of the analyte divided by the fluorescence of just the MB probe in a hybridization buffer following a 30-minute incubation (50 nM MB, 100 nM analytes). The differentiation factor was used to determine the differentiation of wild-type from mutant analyte, and the equation used was Df = 1 − ΔFmm/ΔFm, where ΔF represents the signal of matched (m) or mismatched (mm) analyte with the signal of the blank (no analyte) subtracted. **(C)** The time-dependent hybridization kinetics between analytes and MB1 or MB1-Tail were measured. The analytes were added at the 60s time point, and measurements were resumed at ~75 s, as indicated by the red arrow. **(D)** Initial hybridization rates of 16S analyte with MB1 and MB1-Tail. The line of best fit was used to determine the slope over the first 60 seconds and was taken to be the initial rate of duplex formation.

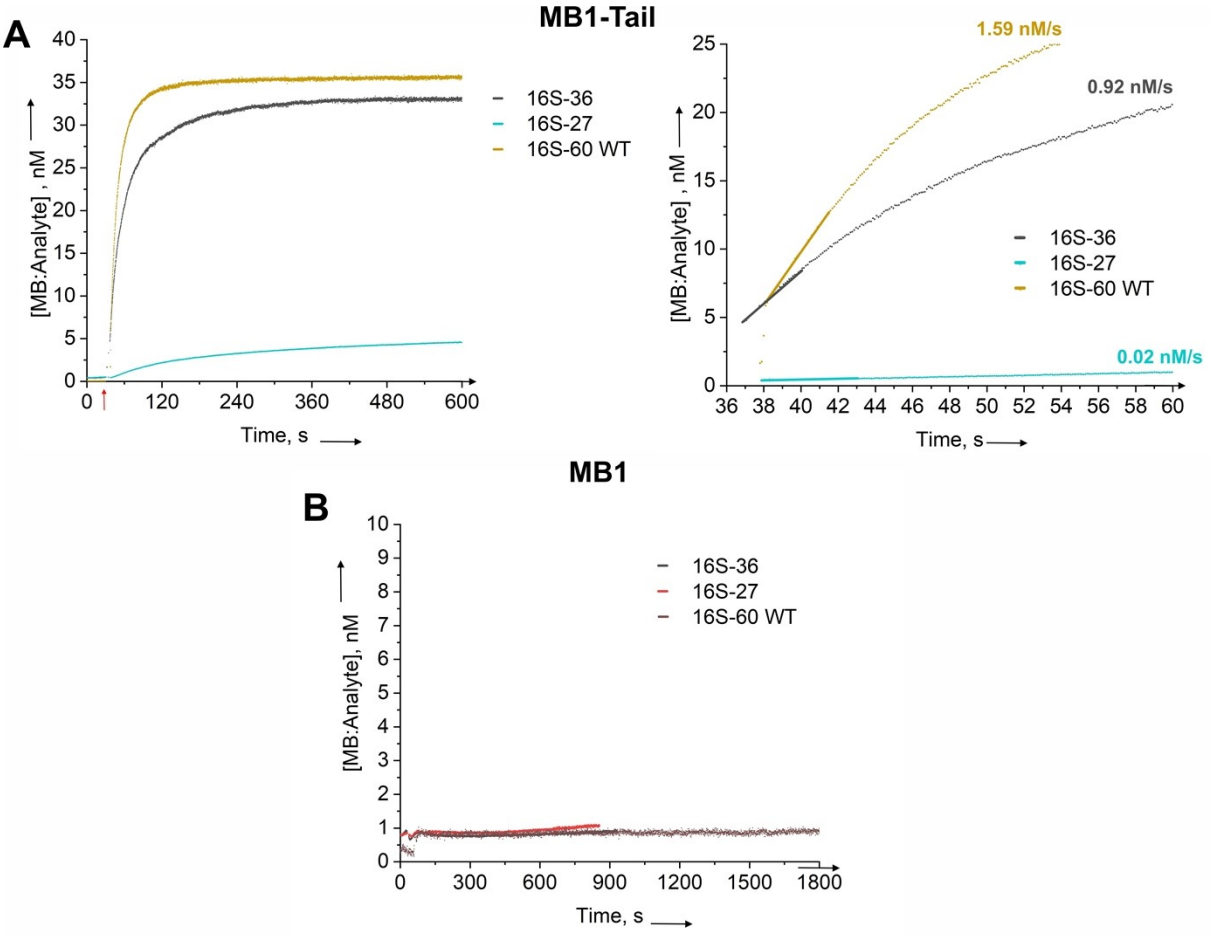

Figure S6. Initial Rate of Hybridization with Shorter 16S Analyte Fragments. MB1-Tail was used with 16S-60 WT analytes and shortened variations to mimic a linear analyte. A) Kinetics between analytes and MB1-Tail (left) over ten minutes and their initial hybridization rates (right) over the first five seconds. The 16S-27 fragment showed a three-fold increase in the initial rate (0.02 nM/s) when compared to the 16S-16 WT fragment (0.007 nM/sec, Fig S2). Although the 16S-60 WT and 16S-36 fragments had the same complementarity to MB1-Tail, 16S-36 had a slower initial hybridization rate (.0.92 nM/sec), which was hypothesized to be due to the possibility of dimer formation for 16S-36, but not 16S-60 WT, at 22 °C. B) Time-Dependence of hybridization between MB1 and analytes showed no appreciable hybridization between analyte and MB probe. Data shown are the average of three independent trials.

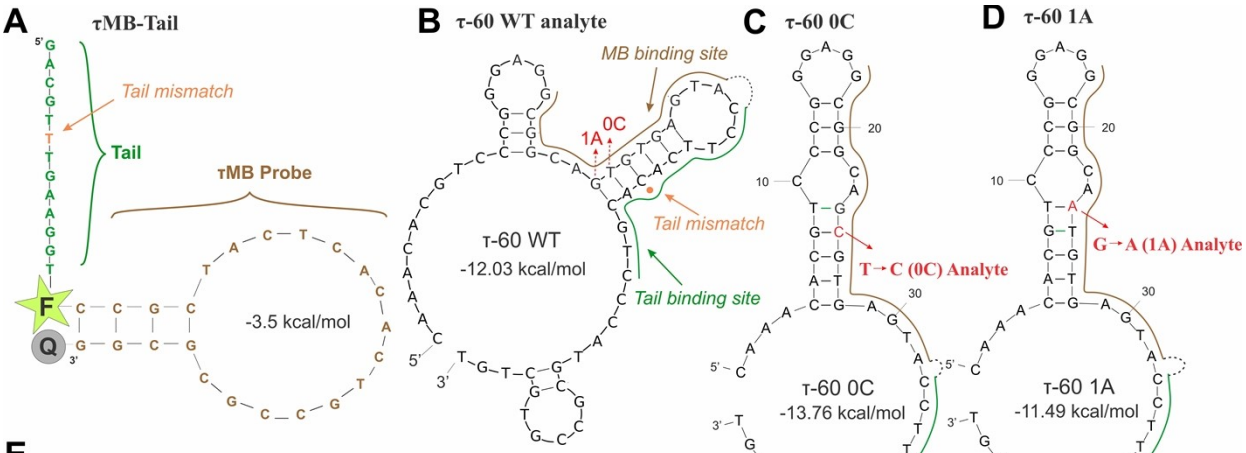

E

ΔG of analyte folding	ΔG of MB Probe/analyte		Change in ΔG upon complex formation	S/B	D_f
τ-60 WT -12.03	τMB-Tail	~ -38.4	~ -22.9	5.2	—
	τMB	~ -28.2	~ -12.7	1.7	—
τ-60 0C -13.76	τMB-Tail	~ -33.6	~ -16.3	11.8	-1.6
	τMB	~ -23.4	~ -6.1	1.6	0.1
τ-60 1A -11.49	τMB-Tail	~ -33.1	~ -18.1	11.3	-1.4
	τMB	~ -22.9	~ -7.9	1.6	0.1

ΔG are in kcal/mol

D_f = 1- (ΔFмм/ΔFм)

Figure S7. Secondary structures of τMB and Tau analytes with quantitative hybridization parameters. **(A)** τMB-Tail has the additional tail outlined in green, τMB outlined in brown, and a mismatch in the tail in blue. **(B)** Secondary structure of τ-60 WT with the tail and MB-binding sites outlined in green and brown, respectively. The SNV-containing analytes 0C and 1A tested are indicated with red arrows in panels (C) and (D). The blue circle represents a mispairing of C:T with T in the tail of the τMB-Tailed probe to prevent unwanted self-complementarity. (E) The free energy associated with each analyte, the complex formed between analyte and probe, the free energy change associated with the formation of the complex, and the differentiation factor for mutant analytes. The signal to background (S/B) was calculated by taking the fluorescent signal at 30 minutes and dividing it by the MB signal. The differentiation factor is calculated with the equation $D_f = 1 - \Delta F_{mm}/\Delta F_m$, where ΔF represents the signal of matched (m) or mismatched (mm) analyte with the signal of the blank (no analyte) subtracted. Due to their secondary structure, the 0C and 1A mutants produced a higher S/B than the WT analyte, resulting in a negative Df. Furthermore, since the assay is performed at 22 °C, we do not expect for our tailed MB probes to be selective, since MB probes typically require higher temperatures to enable them to be selective against SNVs. Compared to the WT analyte, the tail-binding region is mostly contained in a loop, rather than a stem, which allows the tail to easily bind and further facilitate the hybridization of the MB. ΔG values were estimated as described in Fig. 1 legend. ΔG for both τMB and τMB-Tail probes ΔG is –3.49 kcal/mol (not shown in the table). The data are average values of at least 3 independent measurements.

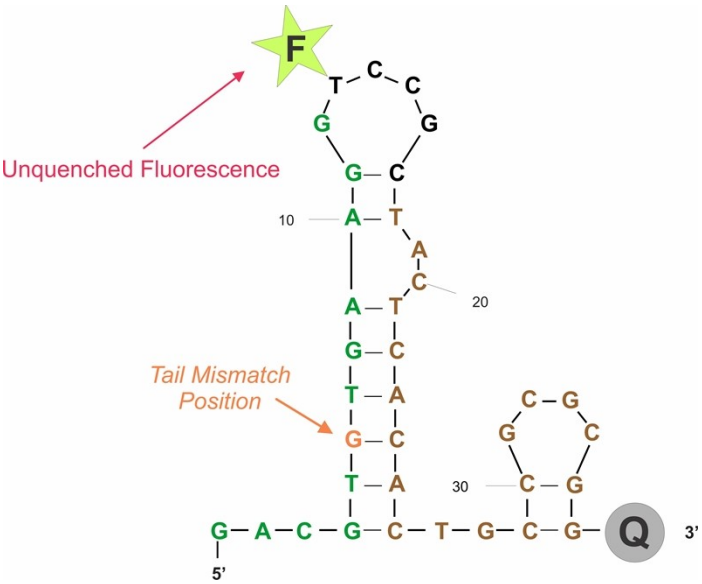

Figure S8. The Tail Invasion Problem in τMB-Tail Without a Tail Mismatch. Without introducing a mismatch in the tail, the MB probe adopts a more stable secondary structure in which the fluorophore cannot be quenched via contact quenching. The secondary structure was predicted using Mfold at 22 °C, $[Na^+]$ = 50 mM, and the $[Mg^{2+}]$ = 50 mM.

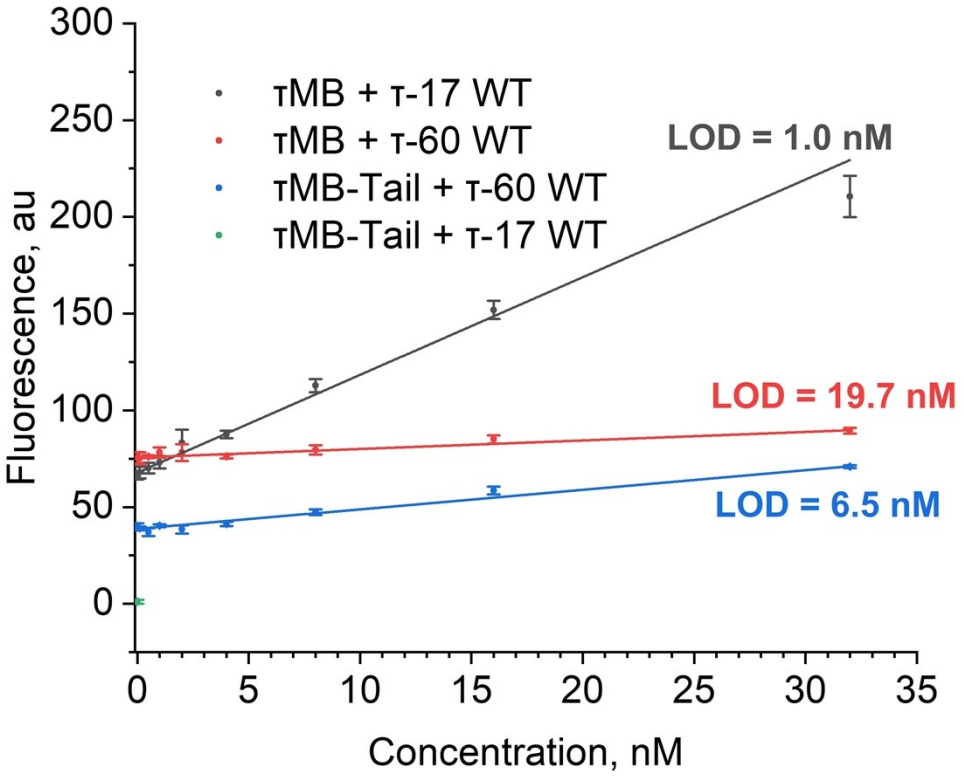

Equation	y = a + b*x			
Plot	τMB + τ-17 WT	τMB + τ-60 WT	τMB-Tail + τ-60 W	τMB-Tail + τ-17 W
Intercept	67.8 ± 1.2	75.6 ± 0.4	38.7 ± 0.5	-- ± --
Slope	5.05 ± 0.21	0.44 ± 0.04	1.01 ± 0.03	-- ± --
Pearson's r	0.99	0.98	1.00	--
R-Square (COD)	0.99	0.96	0.99	--
Adj. R-Square	0.99	0.95	0.99	--

Figure S9 Limit of Detection for τMB-Tail And τMB With Long and Short Tau Analytes. A calibration curve was used to determine the Limit of Detection (LOD) for each analyte by finding the line of best fit. To determine LOD, the average signal of the blank (F0) was added to three times the blank's standard deviation (SD), and this value was used in the line of best fit to solve for x, the lowest detectable concentration of the analyte.

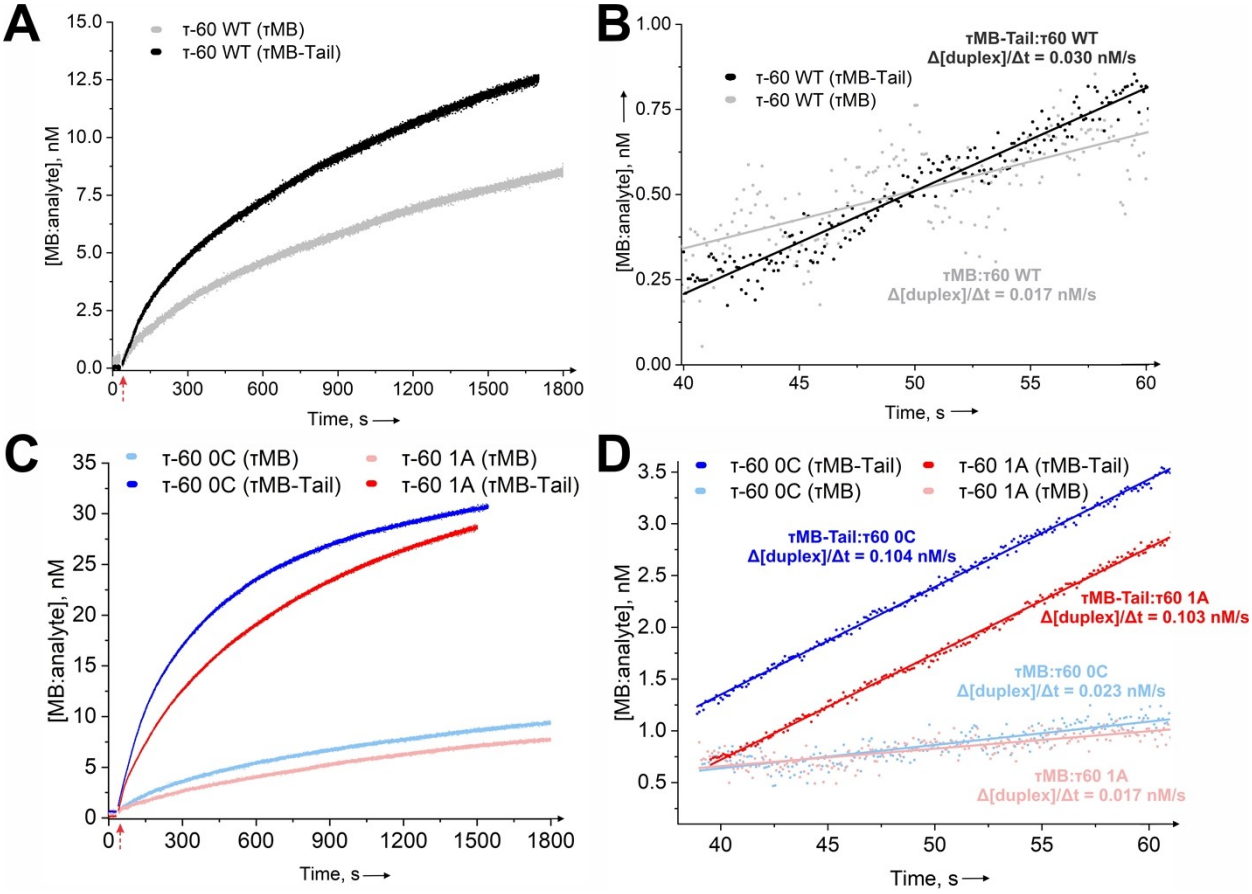

Figure S10. Tailed MB Probe Improves Hybridization Thermodynamics for 60-nt τ Analytes. (A) Time-dependent fluorescent duplex formation between MB probes and matched analytes. The analytes were added at the 30 s time point, indicated by the red arrow, and readings began again at ~40 s. The concentration of MB:Analyte was determined via calibration curves with MB:analyte duplexes (Fig. S12) **(B)** Initial hybridization rates of tau analytes with τMB and τMB-Tail. A line of best fit was determined over the first 20 seconds after analyte addition, and the slope was taken to be the initial rate of duplex formation. **(C)** Time-dependent fluorescent duplex formation for the mismatched τ-60 analytes, 0C and 1A. **(D)** Initial hybridization rates of τ-60 mismatched analytes with τMB and τMB-Tail resulted in a 4.5- and 6.1-fold increase for the 0C and 1A mutants, respectively. Compared to the WT analyte, the faster initial hybridization rates of 0C and 1A mutants can be explained by their secondary structure and the accessibility of ssDNA nucleotides that can readily hybridize with the tail in τMB-Tail and facilitate toehold-mediated hybridization (Fig. S3). The data are average values of at least 3 independent measurements.

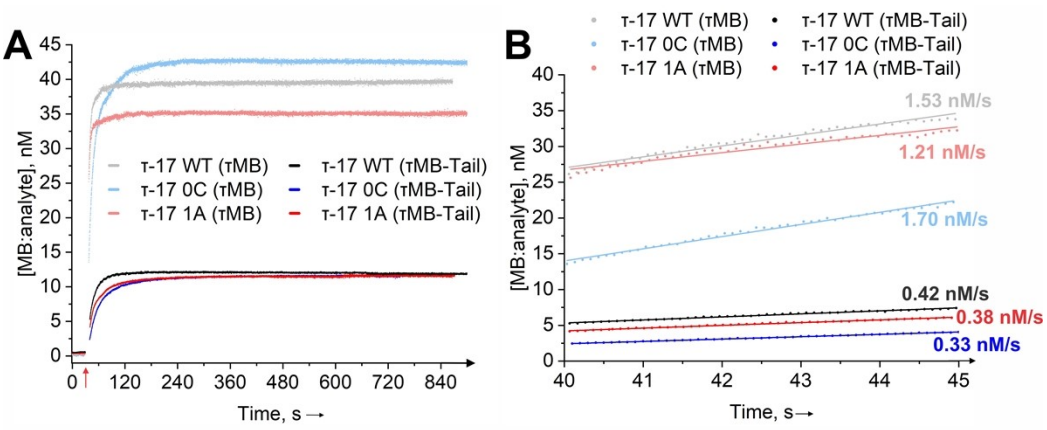

C

ΔG of analyte folding	ΔG of MB Probe/analyte	Change in ΔG upon complex formation	S/B	Initial Rate (nM/s)	D_f
τ-17 WT -0.22	τMB-Tail ~ -24.7	~ -21.0	4.1	0.42	—
	τMB ~ -24.7	~ -21.0	3.4	1.53	—
τ-17 0C -1.88	τMB-Tail ~ -19.9	~ -14.5	3.9	0.33	0.04
	τMB ~ -19.9	~ -14.5	3.5	1.70	-0.06
τ-17 1A -0.82	τMB-Tail ~ -19.4	~ -15.1	4.0	0.38	0.04
	τMB ~ -19.4	~ -15.1	3.0	1.21	0.14

ΔG are in kcal/mol

D_f = 1- (ΔFмм/ΔFм)

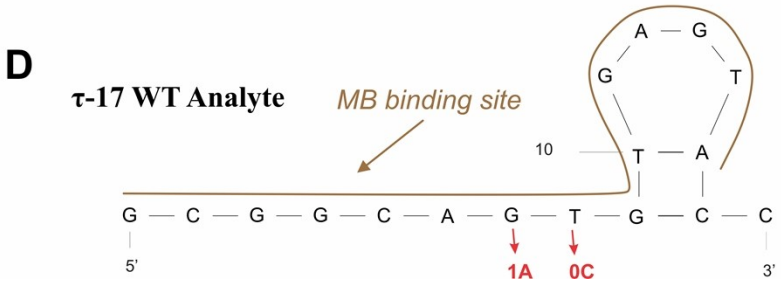

Figure S11. Kinetics and Quantitative data for 17-nt fragments of Tau Analytes. (A) Time-dependent fluorescent duplex formation between MB probes and short tau analytes. The analytes were added at the 30 s time point, indicated by the red arrow, and readings began again at ~40 s. **(B)** Initial hybridization rates of analytes with τMB and τMB-Tail. A line of best fit was determined over the first 5 s after analyte addition, and the slope was taken to be the initial rate of duplex formation. **(C)** The free energy associated with each analyte, the complex formed between analyte and probe, the free energy change associated with the formation of the complex, and the differentiation factor for mutant analytes. The signal to background (S/B) was calculated by taking the fluorescent signal at 30 minutes and dividing it by the MB signal. The differentiation factor is calculated with the equation Df = 1 − ΔFmm/ΔFm, where ΔF represents the signal of matched (m) or mismatched (mm) analyte with the signal of the blank (no analyte) subtracted. ΔG values were estimated as described in Fig. 1 legend. ΔG for both τMB and τMB-Tail probes ΔG is –3.49 kcal/mol (not shown in the table). **(D)** Secondary structure of the τ-17 WT analyte, with the MB binding site outlined in brown and mutations indicated with red arrows.

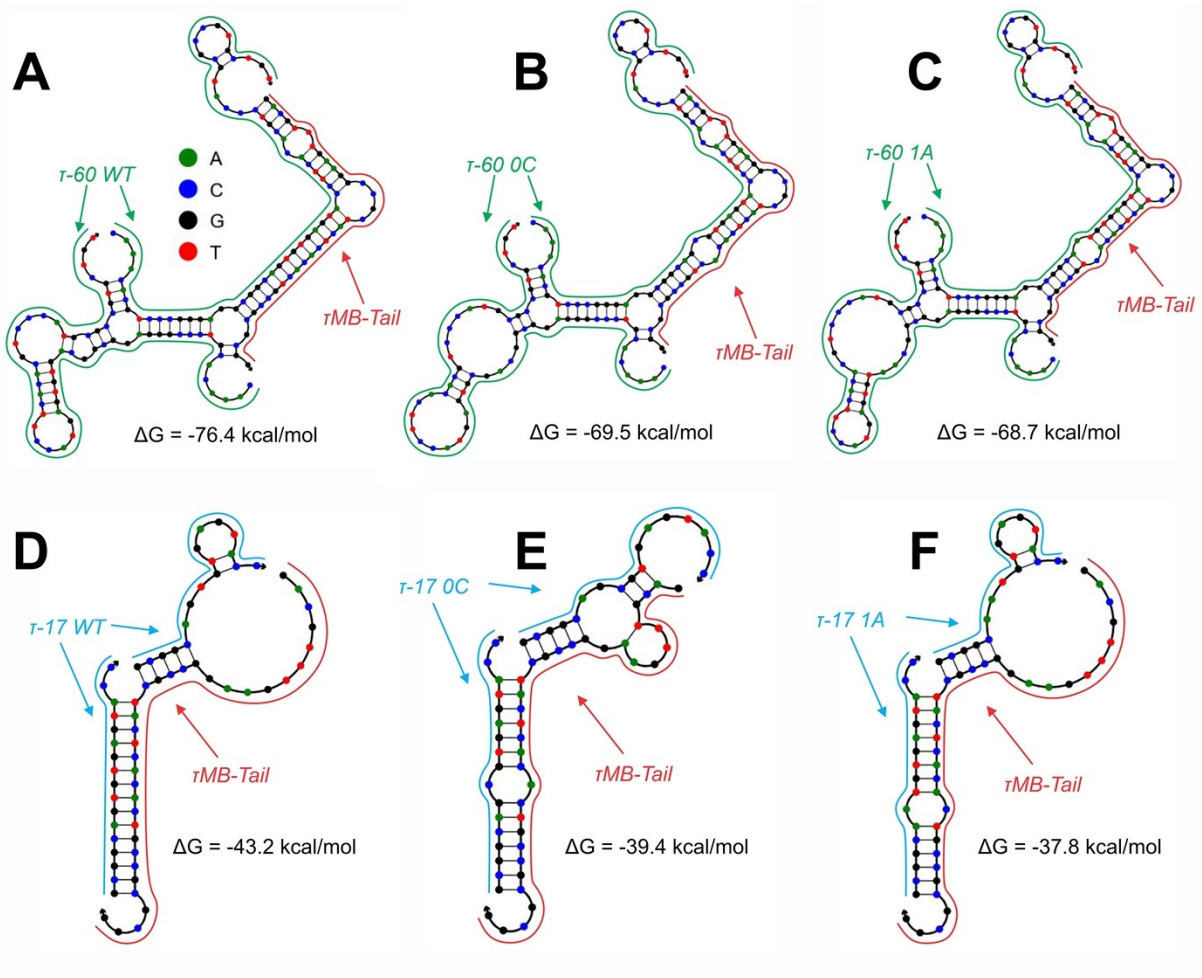

Figure S12. Secondary structures for Tau analytes with τMB-Tail. (A-C) Secondary structures formed upon hybridizing two equivalents of 60 nt analyte with one equivalent of τMB-Tail. **(D-F)** Secondary structures formed upon hybridizing two equivalents of 17 nt analytes with one equivalent of τMB-Tail. Structures and Gibbs energy values (ΔG) were determined using NUPACK at 22 ^{o}C, [Na^{+}] = 50 mM, and [Mg^{2+}] = 50 mM.

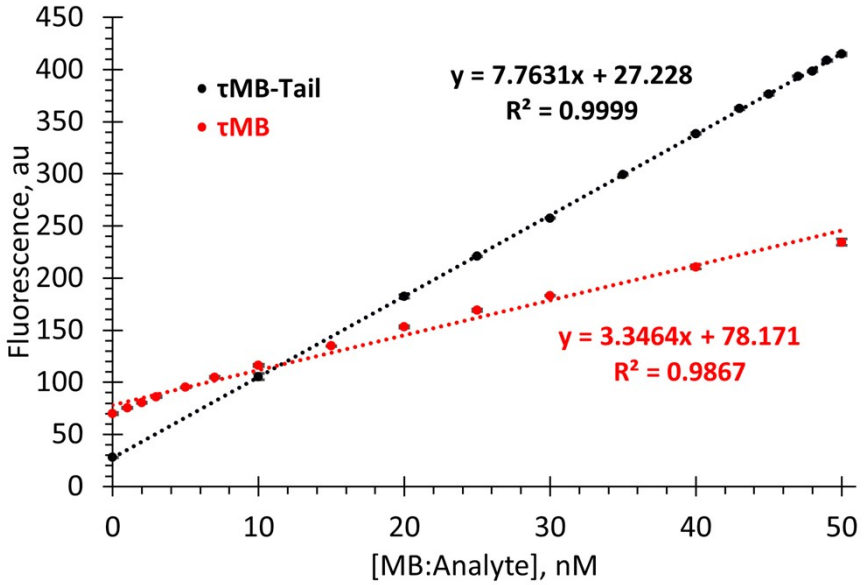

Figure S13. Calibration Curve For Calculation of Kinetic Constants of Hybridization. MB-probe and WT analyte were annealed at a concentration of 100 nM each, heating for 5 min at 95°C and cooling overnight. The concentration of fluorescent duplex was assumed to be 100 nM. Serial dilution was performed to obtain solutions with a concentration of fluorescent duplex 0 – 50 nM. The Fluorescence of each solution was recorded in triplicate, and the line of best-fit and equation of best-fit lines were obtained in Excel. The data are average values of 3 independent measurements.

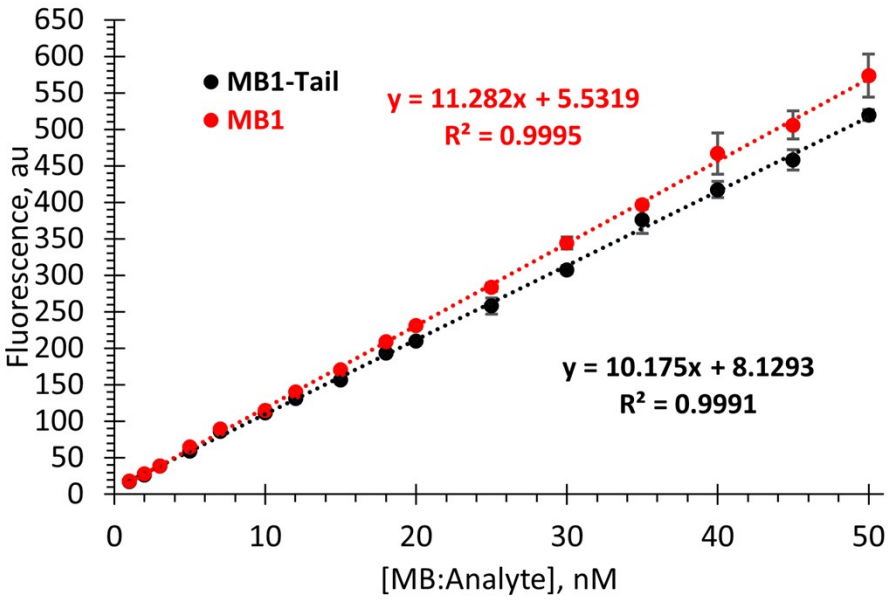

Figure S14. MB1 and MB1-Tail Calibration Curve for Calculation of Kinetic Constants of Hybridization. MB-probe and WT-16 analytes were annealed at a concentration of 100 nM each by heating for 5 min at 95C and cooling overnight. The concentration of fluorescent duplex was assumed to be 100 nM. Serial dilution was performed to obtain solutions with a concentration of fluorescent duplex 0 – 50 nM. The Fluorescence of each solution was recorded in triplicate, and the line of best-fit and equation of best-fit lines were obtained in Excel. The data are average values of 3 independent measurements.

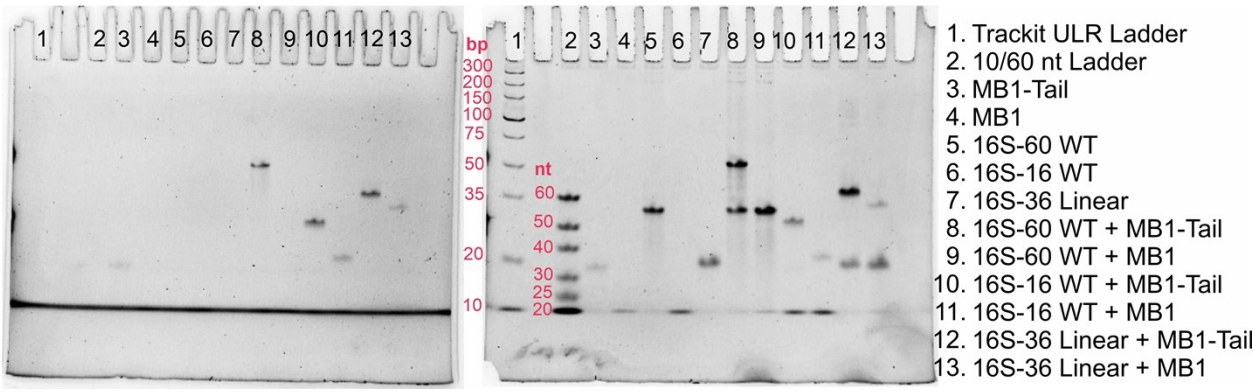

Figure S15. 16S Analyte and MBP Assembly on Native Polyacrylamide Gel Electrophoresis. A 12% Native PAGE without staining (left) and after staining with Gel Red (right) shows the formation of a duplex between 16S-60 WT and MB1-Tail (Lane 8), but not between 16S-60 WT and MB1 (Lane 9). This correlates with the fluorescent data which shows that 16S-60 WT is detectable only when the MB1-Tail probe is used. The gel additionally shows some association between 16S-16 WT and 16S-36 with both MB1 and MB1-Tail (Lanes 10-13). Oligonucleotides were added to the wells in a 2:1 ratio for analyte:MB probe. This gel shows that a complex is formed between 16S-60 WT and MB1-Tail, but not with 16S-60 WT and MB1. These results support our hypothesis that the 'tail' on MB1-Tail is necessary for the hybridziation to the folded 16S-60 WT analyte.

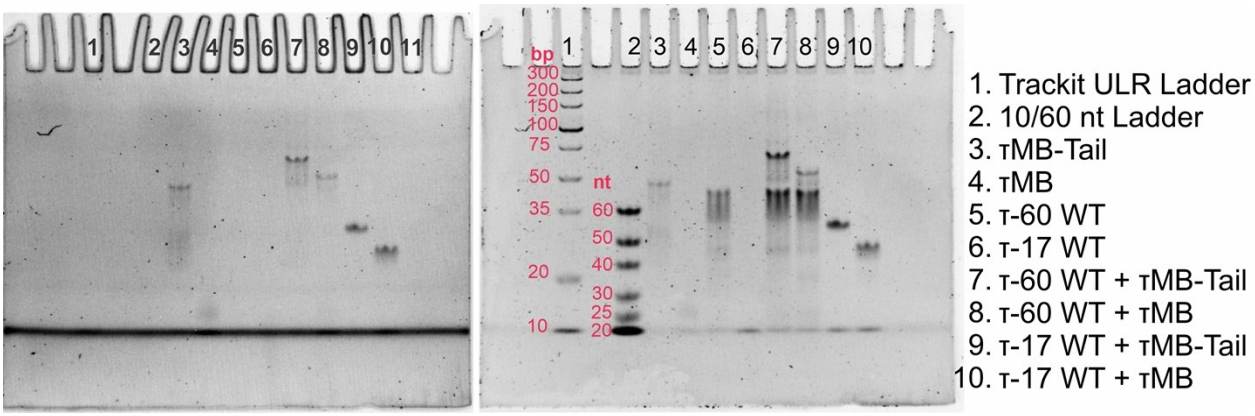

Figure S16. Tau Analyte and MBP Assembly on Native Polyacrylamide Gel Electrophoresis. A 12% native PAGE without staining (left) and after staining with Gel Red (right) shows the formation of a duplex between τ60-WT and τMB-Tail (Lane 7), τ60-WT and τMB (Lane 8), τ17-WT and τMB-Tail (Lane 9), and τ-17 WT and τMB (Lane 10). Oligonucleotides were added to the wells in a 2:1 ratio for analyte:MB probe.

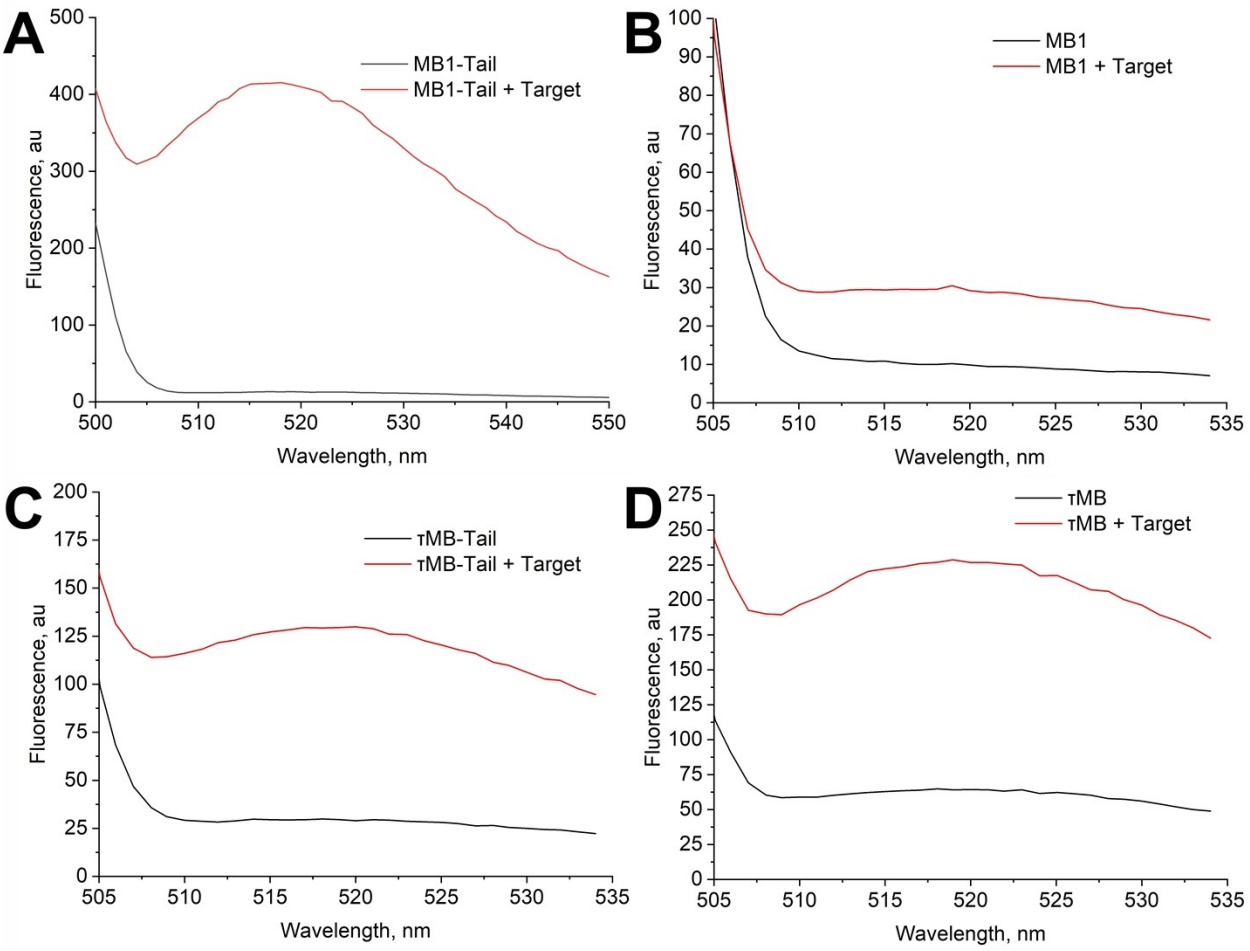

Figure S17. Spectral Profiles for MB Probes. A) MB1-Tail with and without 16S-60 WT analyte. B) MB1 with and without 16S-16 WT analyte. C) τMB-Tail with and without τ-60 WT analyte. D) τMB with and without τ-17 WT analyte. All solutions contained 50 nM MB Probe and, where indicated, 100 nM of target.

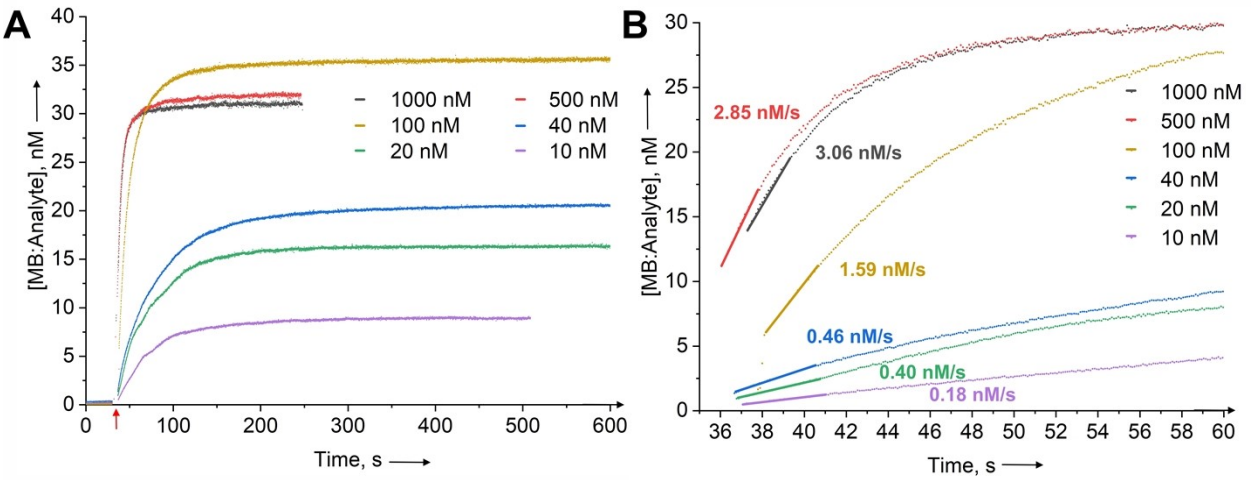

Figure S18. Concentration Dependence of 16S-60 WT with MB1-Tail. A) 10-minute kinetics between 50 nM of MB1-Tail and 16S-60 WT at varying concentrations, with analyte added at the 30s time point, indicated by the red arrow. B) Initial rates of duplex formation between MB1-Tail and 16S-60 WT within the first five seconds. All data shown are the average of three independent measurements. With an 11-bp duplex formed between the tail of the MB probe and the analyte, the initial rate of hybridization is ~1.6 nM/s (16-60 WT). As the complementarity to the tail is reduced to 9 bp, the initial rate of hybridization reduces to 1.3 nM/s (16S T1). With 6 bp (16S T3), the initial rate decreases to 0.07 nM/s, and with three or fewer nucleotides complementary to the tail, the initial rate of hybridization is unable to be determined as hybridization does not occur. Thus, we can conclude that at least six base pairs are needed between the analyte and MB probe tail, but at least nine base pairs are needed to appreciably increase the rate. These findings align with previous studies evaluating the hybridiazation between DNA and its cognate analyte; a full helix, approximately 10 bp, is suitable for fast and efficient hybridization.

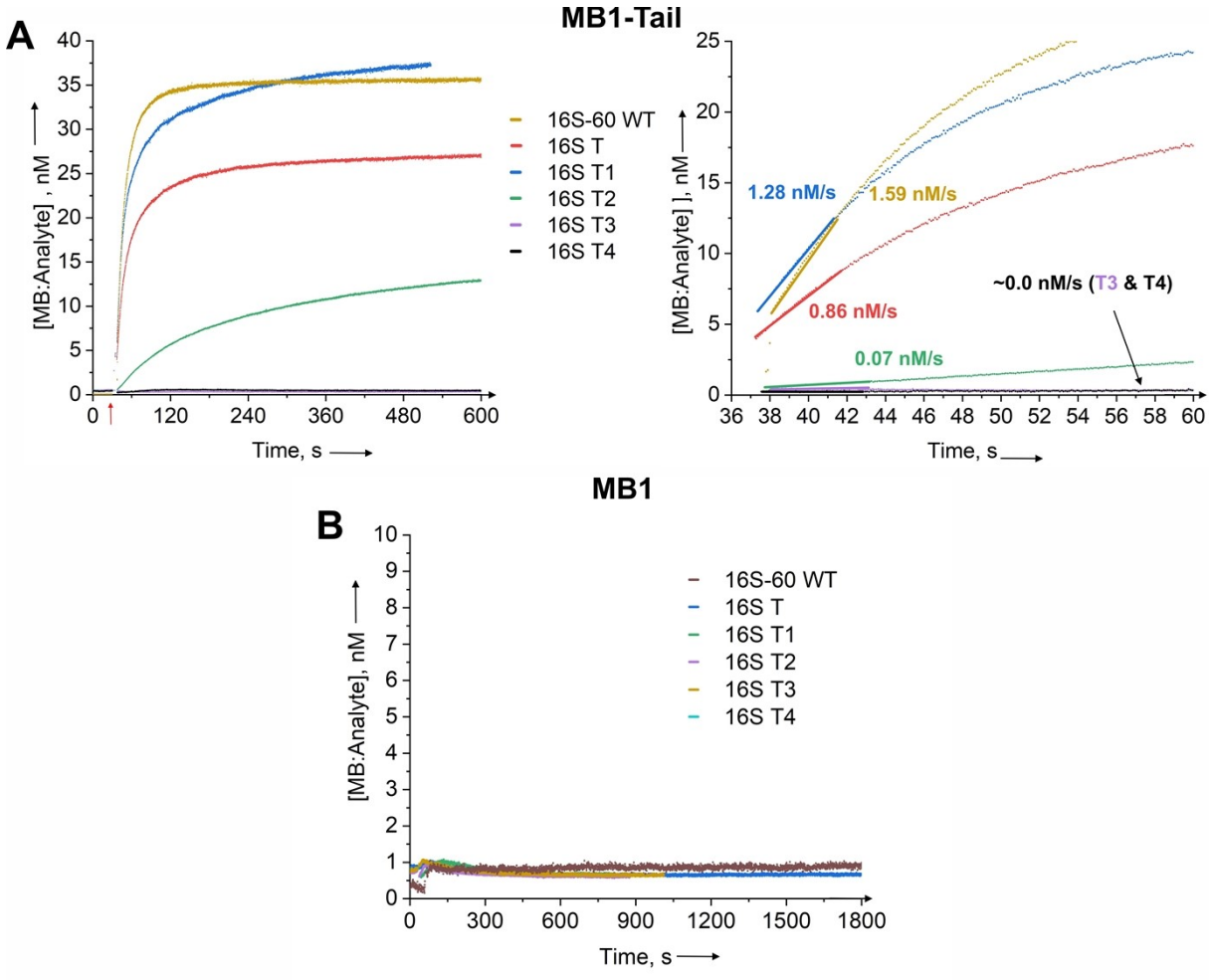

Figure S19. Kinetics of Hybridization between 16S Analytes with Shortened Tail-Binding Regions. MB1-Tail was used with 16S-60 WT analytes and variations which involved shortening the 3'- end to reduce the number of complementary nucleotides between the 'tail' of MB1-Tail and analyte. A) Kinetics between analytes and MB1-Tail (left) over ten minutes and their initial hybridization rates (right) over the first five seconds. B) Time-Dependence of hybridization between MB1 and analytes showed no appreciable hybridization between analyte and MB probe. Data shown are the average of three independent trials.

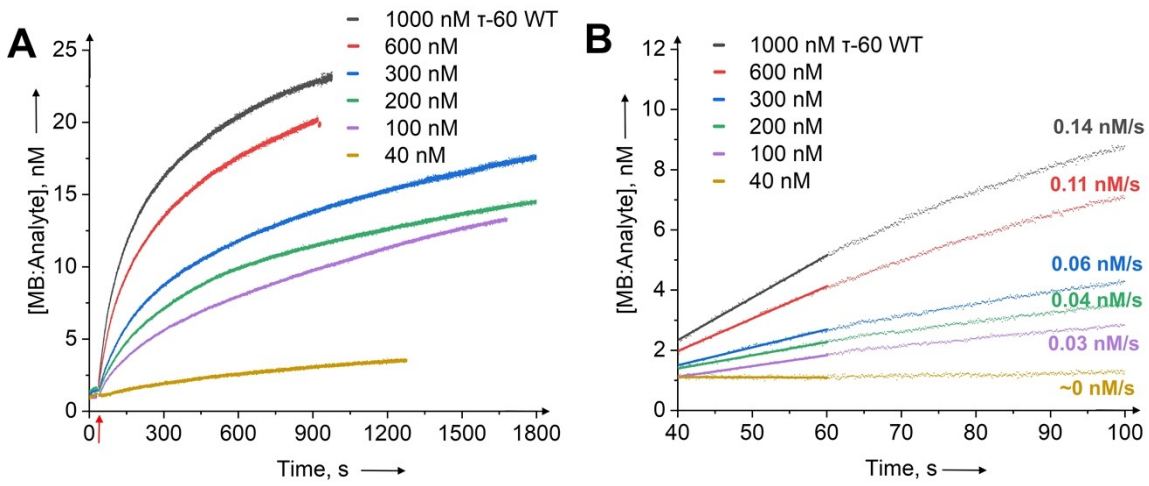

Figure S20. Concentration Dependence of τ-60 WT with τMB-Tail. A) Kinetics between 50 nM τMB-Tail and τ-60 WT at varying concentrations, with analyte added at the 30s time point, indicated by the red arrow. B) Initial rates of duplex formation between τMB-Tail and τ-60 WT within the first twenty seconds. All data shown are the average of three independent measurements.

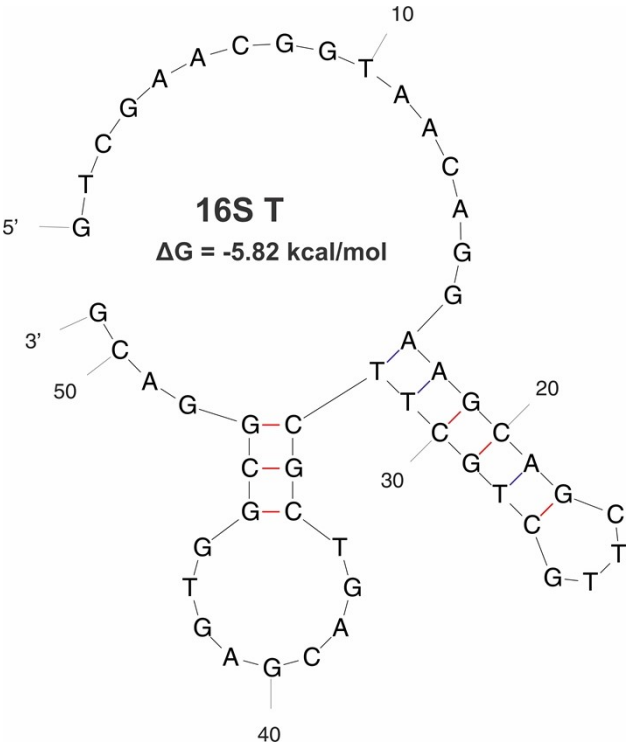

Figure S21. Secondary structure of 16S T. The secondary structure of 16S T can lead to decreased hybridization rates, as found in Fig. S20. The Gibbs energy values (ΔG) and secondary structure was obtained at 22 °C, $[Na^+]$ = 50 mM, and the $[Mg^{2+}]$ = 50 mM using Mfold.